

LOW FREQUENCY ACOUSTIC TRANSMISSION THROUGH THE WALLS OF RECTANGULAR DUCTS†

A. CUMMINGS

*Institute of Environmental Science and Technology, Polytechnic of the South Bank,
London SE1 0AA, England*

(Received 15 April 1978, and in revised form 20 July 1978)

A simple theory is described for the transmission of low frequency sound through the walls of rectangular ducts, particularly those in air conditioning systems. The model is based on a coupled acoustic/structural wave system, and it is assumed that the duct radiates in the same way as a finite-length line source incorporating a single travelling wave. Measurements of wall transmission loss on two types of duct system are compared to theoretical predictions, and good agreement is obtained within the frequency range of validity of the theory. It is concluded that the present approach should give reliable estimates of noise transmission in practical situations.

1. INTRODUCTION

The engineer who is involved in carrying out acoustical design work on buildings is usually faced, sooner or later, with the problem of estimating the extent of noise transmission from the interior to the exterior of air-moving ductwork in a ventilating system. This is sometimes necessary where, for example, a duct passes through a space which is not actually served by the duct system; since noise from an air-handling fan would normally be transmitted along the duct, one would expect the duct walls to vibrate, thus radiating noise into the intermediate space. Now if a silencer were placed adjacent to the fan but designed solely on the basis of duct-borne fan noise transmitted via air outlets to the spaces which they serve, the intermediate duct-wall radiation would be ignored, and acoustic problems could arise in the intermediate space, despite the presence of the attenuating device. So one should, perhaps, account for duct-wall radiation as part of a noise transmission path. In practice, this effect *can* be troublesome and the phenomenon of acoustic transmission through duct walls is known colloquially, in the air conditioning fraternity, as “breakout” (although one feels that this term has a somewhat inappropriate flavour). A good account of breakout is given by Webb [1].

It is clear then, that one stock-in-trade of the engineer concerned with building acoustics must be a reliable means of estimating noise breakout from ductwork.

Breakout, it would seem, is predominantly a low frequency problem, since fans produce most of their sound power at low frequencies, and it is also in this region where the almost universally used dissipative type of attenuator is at its least effective. Hence one's breakout calculations should be valid at low frequencies; high frequency accuracy is less important.

At this point, it must be mentioned that duct-wall vibration may be excited by flow turbulence as well as by acoustic pressure waves. Webb discusses this phenomenon in

† A version of this paper was given at the Spring meeting of the Institute of Acoustics, at the University of Cambridge, 5–7 April, 1978.

reference [1]; it appears that it is most likely to be important in high velocity ductwork, or where there are obstacles in the flow such as dampers or internal reinforcing members. Additionally, there is the possibility of instability caused by the *interaction* between wall vibration and a "clean" air flow (although clean air flows are unlikely to occur in any practical ventilating system). It is not the purpose of this article, however, to discuss aerodynamic excitation of duct walls: here, only acoustic forcing will be considered. This mode of transmission is probably of at least equal importance to that associated with turbulence, and in any case, the latter could prove difficult to estimate numerically since the necessary detailed information on the wall pressure field, caused by turbulence only, would not normally be available.

Air-moving ductwork has three principal cross-sectional shapes: circular, oval (with flat sides) and rectangular. The extent of acoustic radiation from the walls, and also even its *mechanism*, may vary from one shape to another.

Consider first circular ducts. High frequency transmission through circular section duct walls has been studied by Cremer [2] and Heckl [3], with some degree of success. But, since it is not the high frequency region (where many acoustic modes propagate in the duct) which is of concern here, this work has little relevance in the present context. Morfey [4], Brown and Rennison [5], and Kuhn and Morfey [6] have all examined low frequency transmission through the walls of circular pipes. The overall conclusions to be drawn from these three pieces of work are (i) that it is possible to calculate low frequency transmission by *axisymmetric* pipe vibrations only—fairly easily and accurately, and (ii) (from reference [6]) that in practical situations axisymmetric duct-wall radiation is not likely to be the major transmission mechanism in circular metal ducts, but that bending wave radiation from the duct as a *whole* (excited by non-axisymmetric pressures at some point(s) inside the pipe) would probably dominate! Since the chances of one's knowing the magnitudes and distributions of the exciting forces are extremely remote, this means that there is little hope of calculating the low frequency radiation from circular ductwork. One happy feature of the situation is, however, that low frequency breakout from circular ducts is not normally too much of a problem, since the low frequency transmission loss (a definition of which will be given later) of the duct walls tends to be high, even when the bending mode mechanism predominates.

Oval ducts could not vibrate axisymmetrically, and the wall transmission loss would be considerably less than that of circular ducts (for reasons which are obvious from reading references [4–6]). Quite possibly, noise transmission from "peristaltic" wall vibrations would dominate, in this case, over whole-duct bending mode radiation. But oval ducts are, it would seem, less commonly occurring than either circular or rectangular ducts and attention will not, at present, be focussed upon them.

So the subject of interest in this article is low frequency noise breakout from *rectangular* ducts.

As far as can be ascertained, no method of estimating noise breakout from rectangular ducts at low frequencies is currently available. A very simple formula quoted by Allen [7] is frequently used for the purpose, but it is, unfortunately, only likely to have any degree of success at all at *high* frequencies (it is based on the idea of multi-mode duct transmission) and even then is probably not reliable: Allen, in reference [7], says, "... the *TL* of the duct wall may be assumed to approach the field mass law . . . although there may be wide departures from these values." As is common with simplistic formulae, Allen's is widely misused, and is certainly totally inapplicable at low frequencies where only single mode transmission occurs in the duct. (Incidentally, Webb [1] appears to be incorrect in describing Allen's formula as an "empirical equation".)

The purpose of the present work is to attempt to evolve a reasonably simple, but reliable,

means of estimating noise breakout from rectangular ducts. Mean fluid flow Mach numbers in air conditioning ducts are small enough to be negligible, and so flow will not be taken into account in the ensuing discussions.

2. THEORY

Consider an infinitely long duct of rectangular, uniform cross-section, with uniform flexible walls whose thicknesses are all equal (it is not worthwhile to account for the unusual situation where the walls have different thicknesses, although this would involve no additional difficulties), and which contains negligible mean fluid flow. The fluid properties inside and outside the duct may differ, and are characterized by the density ρ and the adiabatic speed of sound c . The situation is illustrated in Figure 1, which also shows a set

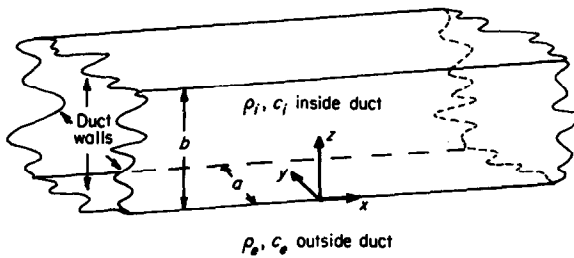


Figure 1. Rectangular duct.

of Cartesian co-ordinates; the subscripts i and e on ρ and c indicate properties of the internal and external fluids respectively (also a list of symbols is given in the Appendix).

Such a duct contains most of the essential features of a typical air-moving duct. The problem now resolves itself into examining first, the internal sound propagation and resultant wall vibration, including the way in which the fluid wave and the structural wave couple together, and secondly the external acoustic radiation from the duct walls. Because the frequency is assumed to be low, certain convenient approximations may be made. The first of these is that the sound field inside the duct consists of a travelling wave with an approximately uniform acoustic pressure distribution. This would be exactly true for the fundamental mode in a rigid-walled duct, but is not a bad approximation for the fundamental mode in ducts with yielding walls, provided the wall admittance is not too large. The second assumption is that the acoustic wavelength c_e/f (where f is the frequency) is fairly large compared to the larger transverse duct dimension (the ratio should be, say, greater than 2:1). The latter requirement is virtually guaranteed to be satisfied by the former. An additional assumption will be that the external radiation load on the duct walls has little effect on the wall vibrations (one thus avoids the considerable complication of including the external pressure field in an analysis of the duct wall vibrations). This will be valid provided the duct walls are not too "transparent" to sound. One should first derive an acoustic wave equation for the sound field inside the duct.

2.1. ACOUSTIC WAVE EQUATION

It is required to derive a wave equation for approximately one-dimensional sound propagation in a uniform duct with yielding walls. The cross-sectional shape may be arbitrary: the cross-sectional area is denoted by S and the perimeter by L . Figure 2 illus-

trates such a duct; a co-ordinate around the perimeter is denoted by s , and the axial co-ordinate by x . A thin, transverse fluid element, of thickness Δx , is shown.

If the normal admittance of the duct walls (non-dimensionalized against $\rho_i c_i$) is $\beta(s)$, and an average admittance $\bar{\beta}$ is defined

$$\bar{\beta} = \frac{1}{L} \int_0^L \beta(s) ds, \quad (1)$$

one may balance the total net mass flow into the element, $-(\rho_i S \hat{c} u_x / \partial x + p L \bar{\beta} / c_i) \Delta x$,

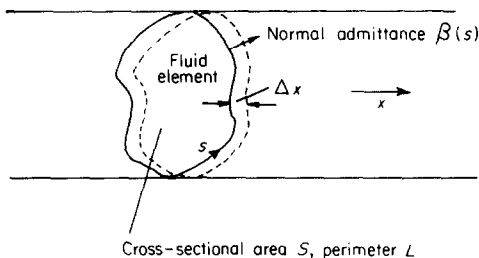


Figure 2. Duct with yielding walls.

against the rate of increase of mass of fluid in the element, $S \Delta x \hat{c} \rho / \partial t$ (u_x , p and ρ are axial acoustic particle velocity, pressure and density respectively), and allow Δx to tend to zero, to obtain a continuity equation

$$(\partial \rho / \partial t) + \rho_i (\partial u_x / \partial x) + (p L \bar{\beta} / c_i S) = 0. \quad (2)$$

The momentum equation, expressing the force balance on the element, is

$$\rho_i \partial u_x / \partial t = -\partial p / \partial x. \quad (3)$$

and equations (2) and (3) may be combined to give a wave equation,

$$(1/c_i^2)(\partial^2 p / \partial t^2) + (L \bar{\beta} / c_i S)(\partial p / \partial t) - (\partial^2 p / \partial x^2) = 0. \quad (4)$$

If one takes simple harmonic pressure fluctuations, with $p(x, t) \propto e^{i\omega t + \lambda x}$ (ω = radian frequency), equation (4) yields

$$\lambda = \pm i k_i (1 - (i L \bar{\beta} / k_i S))^{1/2} \quad (5)$$

(where $k_i = \omega / c_i$), or, if $\lambda = -i k_x$, then the axial wavenumber k_x is given by

$$k_x = \mp k_i (1 - (i L \bar{\beta} / k_i S))^{1/2}. \quad (6)$$

The positive sign in equation (6) represents a wave travelling in the positive x -direction, and the negative sign denotes a negative-travelling wave.

The foregoing expressions are valid provided the pressure distribution in the duct is nearly uniform, which means that the wall admittance should be fairly small.

2.2. STRUCTURAL WAVE EQUATION

For a thin plate in the x - z plane (for example) of Figure 1, the wave equation for simple harmonic vibrations may be written as

$$(\nabla^4 - \gamma^4)\xi = Kq, \quad (7)$$

where $\nabla^4 \equiv (\partial^2 / \partial x^2 + \partial^2 / \partial z^2)^2$, ξ is the transverse plate displacement from equilibrium (in

the y -direction), $K = 12(1 - \sigma^2)/Eh^3$, E being the Young's modulus of the plate, h the plate thickness and σ Poisson's ratio for the plate material, $\gamma^4 = \omega^2 mK$, m being the mass per unit area of the plate, and q is the forcing pressure (that is, the pressure difference between the two sides of the plate). Both ξ and q may be functions of x and z .

Now since it has been assumed that the acoustic pressure inside the duct is uniform, and also that the radiation load on the outside of the duct is negligible (that is, the plate behaves as if one side is *in vacuo*), q is now only a function of x and may be replaced by $Q(x)e^{i\omega t}$. Also the operator $(\nabla^4 - \gamma^4)$ in equation (7) may be factorized, and if $\xi(x, z, t)$ is replaced by $D(x, z)e^{i\omega t}$, then the equation becomes

$$(\nabla^2 + \gamma^2)(\nabla^2 - \gamma^2)D = KQ. \quad (8)$$

This equation governs the wave motion of the duct wall in the x - z plane, and also in the wall opposite this; if z is replaced by y in the above lines, then it would apply to the x - y walls, where $D(x, y)$ would be the displacement amplitude in the z -direction.

If internal damping in the wall material is to be accounted for, then the Young's modulus E may be replaced by a "dynamic modulus", $E(1 + i\eta)$, where η is the "loss factor" of the material.

2.3. COUPLING BETWEEN ACOUSTIC AND STRUCTURAL WAVES

It is clear from equation (6) that the axial wavenumber of the acoustic wave is dependent upon the wall impedance $\bar{\beta}$; this means that the wall vibrations influence the acoustic propagation. That the reverse is also true may be inferred from equation (8) since Q , the forcing function, is nothing other than the acoustic pressure in the duct. So the fluid-borne and structure-borne waves are interdependent, coupled, waves, both with the *same* axial wavenumber. The next step now is to solve the structural wave equation, with use of this knowledge; the average wall admittance, $\bar{\beta}$, can then be determined as a function of k_x , and the resultant equation, with equation (6), form together a set of two coupled equations from which k_x may be determined. The values of k_x which will be sought are those not *too* far removed from $\pm k_z$; this arises from equation (6), since the wall admittance is assumed to be fairly small.

2.4. SOLUTION OF THE STRUCTURAL WAVE EQUATION

In the last section, it has been mentioned that the structural- and fluid-borne waves have the same axial wavenumber, and that the forcing function $Q(x)$ in equation (8) is the acoustic pressure inside the duct. Now Q is equal to $P_0 e^{-ik_x x}$, where P_0 is the internal pressure amplitude, and so D in equation (8) must have the form $Z(z)e^{-ik_x x}$ for the x - z walls of the duct, and $Y(y)e^{-ik_x x}$ for the x - y walls.

Equation (8) may be solved exactly for a single travelling mode: the particular integral (PI) is equal to $KP_0 e^{-ik_x x}/(k_x^4 - \gamma^4)$, and the complementary function (CF) is given, for the x - y walls, by

$$CF = [A_1 \cos(\alpha_1 y) + A_2 \sin(\alpha_1 y) + A_3 \cosh(\alpha_2 y) + A_4 \sinh(\alpha_2 y)] e^{-ik_x x} \quad (9)$$

and for the x - z walls, by

$$CF = [B_1 \cos(\alpha_1 z) + B_2 \sin(\alpha_1 z) + B_3 \cosh(\alpha_2 z) + B_4 \sinh(\alpha_2 z)] e^{-ik_x x}, \quad (10)$$

where

$$\alpha_1 = \sqrt{\gamma^2 - k_x^2}, \quad \alpha_2 = \sqrt{\gamma^2 + k_x^2} \quad (11a, b)$$

and the constants A_1 to A_4 and B_1 to B_4 are determined by boundary conditions. The general solution is equal to $(PI + CF)$ for the x - y and the x - z walls. The first two terms in each of the brackets in equations (9) and (10) represent solutions to the equation $(\nabla^2 - \gamma^2)D = 0$, and the second two terms represent solutions to $(\nabla^2 + \gamma^2)D = 0$.

The general solutions to equation (8), for the x - y and x - z walls, respectively, are now

$$\begin{aligned}
 D(x, y) &= [A_1 \cos(\alpha_1 y) + A_2 \sin(\alpha_1 y) + A_3 \cosh(\alpha_2 y) + A_4 \sinh(\alpha_2 y)]e^{-ik_x x} \\
 &\quad + [KP_0/(k_x^4 - \gamma^4)]e^{-ik_x x}, \\
 D(x, z) &= [B_1 \cos(\alpha_1 z) + B_2 \sin(\alpha_1 z) + B_3 \cosh(\alpha_2 z) + B_4 \sinh(\alpha_2 z)]e^{-ik_x x} \\
 &\quad + [KP_0/(k_x^4 - \gamma^4)]e^{-ik_x x}.
 \end{aligned}
 \tag{12a, b}$$

2.5. APPLICATION OF BOUNDARY CONDITIONS

Provided one can determine the values of the coefficients in equations (12), then the average wall admittance, $\bar{\beta}$, may be found by using equation (1).

It will be assumed here that (i) the normal wall displacement at a corner of the duct is zero, (ii) the duct corners remain right-angled (meaning that the transverse slopes of adjacent sides, at the corners, differ by 90°) during a vibration cycle, but may rotate in a plane normal to the duct's axis, and (iii) the duct's walls vibrate symmetrically about two planes, each parallel to one set of walls and bisecting the other set. Assumption (i) is valid, since the walls will not undergo significant extensional vibrations. Assumption (ii) is quite reasonable, and is usual in structural vibration problems. Assumption (iii) is justifiable on the basis that, because of the (assumed) uniform pressure fluctuations inside the duct, there should be no asymmetry in the wall vibrations. If the duct were *square* in cross-sectional shape, then the walls would all vibrate in phase, and with equal amplitude at equivalent points. Since the duct is not necessarily assumed to be square, one must allow for rotation of the corners, and require that only *opposite* walls vibrate equally.

On the basis of the three above assumptions, a set of boundary conditions may be drawn up, from which the constants in equations (12) may be found. These only need be applied (in view of the foregoing comments) to two adjacent walls, which are chosen as those in the x - y and x - z planes. The boundary conditions are as follows (the Roman numerals denote which of the above assumptions leads to the particular boundary condition, and a and b are the transverse dimensions of the duct in the y and z directions respectively):

$$(i) \quad Y(0) = 0, Z(0) = 0, Y(a) = 0, Z(b) = 0, \tag{13a-d}$$

$$(ii) \quad Y'(0) = -Z'(0), Y'(a) = -Z'(b), \tag{13e, f}$$

$$(iii) \quad Y'(a/2) = 0, Z'(b/2) = 0, \tag{13g, h}$$

where the primes denote differentiation with respect to argument. The last two conditions are not strictly boundary conditions but arise from the symmetry of the wall vibrations.

Equations (13) give rise to a set of linear equations which may be solved simultaneously to give the coefficients in equations (12) in terms of P_0 .

2.6. TRANSMISSION LOSS OF DUCT WALLS

The term transmission loss (TL), in this context, departs slightly from its usual meaning (which is the decibel ratio between incident and transmitted sound power through equal

areas of a "transmission system" (as, for example, in the case of an infinite partition)—or between *total* incident and transmitted power—as in the case of a duct silencer), since (for a *finite* duct) the total external radiating area of the duct depends upon its length, and hence a *TL* defined as incorporating duct length is not a unique function of the duct geometry and material. But, as will be seen, the duct length affects the acoustic radiation *efficiency*, and so if the *TL* were defined in terms of radiation from a unit length of duct, one would still not have a unique function of duct geometry and wall material. On the other hand it turns out that, over much of the frequency range, the *TL*, defined in terms of radiated sound power per unit length, is only weakly dependent upon the duct's radiating length, and so it is probably more useful to use this type of definition in this case, since the inclusion of a term $10 \log(\text{duct length})$ is sufficient to enable one to calculate the total sound power radiated from any length of duct.

Accordingly, the *TL* will be defined as

$$TL = 10 \log(W_{\text{int}}/W_{\text{rad}}), \quad (14)$$

where W_{int} is the total sound power being transmitted *inside* the duct (this is assumed to be independent of distance along the duct; in reality, W_{int} would slowly decrease in the direction of propagation, because of external radiation losses) and W_{rad} is the radiated sound power per unit length of duct. The above definition contrasts with the more usual one (see, for instance, reference [6]), where W_{rad} is the *total* sound power radiated from the duct.

To calculate the *TL*, one must first estimate the wall response to the internal sound pressure field. This may be done by using equations (12) and (13). The next aspect of the problem is to calculate the radiated sound power from the duct walls.

To carry out a thorough analysis of acoustic radiation from the duct's walls would be unduly complicated, but since the acoustic wavelength has been assumed to be reasonably long compared to the transverse dimensions of the duct, one may, as a first approximation simply integrate the surface velocity amplitude around the duct walls, and use the resulting *volume* velocity per unit length to estimate radiation based on a line source model. This approach would, of course, only really be valid at low frequencies where scattering effects are small and phase differences between the contributions—to the direct external acoustic field at a particular point—from different regions around the duct's perimeter may be neglected.

Brown and Rennison [5] use an extremely simple model in their work on circular pipes. The model consists of a finite length of straight pipe down which axisymmetric, peristaltic waves travel *in one direction only*. The total sound power radiated from this pipe, into a free field, is readily calculated in terms of the pipe's radius, the axial wavenumber, the surface velocity amplitude and the length of the pipe. No "end effects" are assumed to affect the wave propagation, which is taken as that which would occur for a travelling mode in an infinite pipe.

What is gratifying about Brown and Rennison's model is that they find that it gives good predictions of radiation efficiency, not only for an anechoically-terminated duct (the term referring to both acoustic and structural waves), but also for a duct in which waves propagate in *both* directions. Because of its successful application in reference [5], this approach will be used here, although the radiated sound power will be expressed in terms of volume velocity instead of pipe-wall velocity.

One may easily show that the sound power per unit length, radiated from an infinitely long line source down which waves travel with *supersonic* phase speed (referred to c_e), is

$$W_{\text{rad}} = \omega \rho_e |q_0|^2 / 8, \quad (15)$$

where q_0 is the volume velocity amplitude per unit length of duct.

For a finite length of duct, W_{rad} may be expressed in terms of equation (15), incorporating a "radiation efficiency" factor C_r :

$$W_{rad} = C_r \omega \rho_e |q_0|^2 / 8. \tag{16}$$

Brown and Rennison's paper contains a graph (their Figure 3) from which C_r may readily be calculated in terms of the parameter $lk_x(1 - k_e/k_x)$, where l is the length of the duct and $k_e = \omega/c_e$. (If k_x has a small imaginary part—which it will if $\eta \neq 0$ —then the *real* part would be used here.) If $k_x = k_e$ (that is, the duct waves travel at the external acoustic speed), then $C_r = 0.5$, and is independent of l . Provided k_x is not too different from k_e , C_r would be fairly close to 0.5 if $k_x l$ is not too great. A curve of C_r , derived from Brown and Rennison's paper, is given in Figure 3

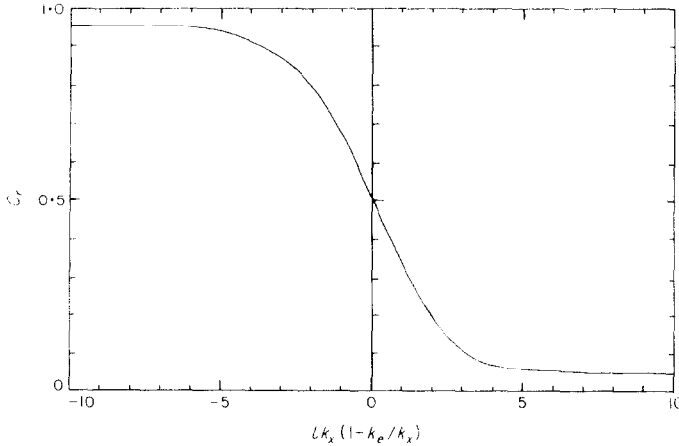


Figure 3. Radiation efficiency of a finite length line source.

The volume velocity q_0 , in equation (16), may be expressed in terms of the wall admittance as

$$q_0 = (2P_0/\rho_i c_i)(a\bar{\beta}_y + b\bar{\beta}_z), \tag{17}$$

where $\bar{\beta}_y$ and $\bar{\beta}_z$ are the average admittances over the x - y walls and the x - z walls respectively.

The internal sound power, W_{int} , is equal to $ab|P_0|^2/2\rho_i c_x$, where c_x is the (real) axial phase speed of the wave, and so the TL may be expressed (by using equations (16) and (17)) as

$$TL = 10 \log(ab\rho_i c_i / C_r k_i \rho_e c_x |a\bar{\beta}_y + b\bar{\beta}_z|^2). \tag{18}$$

The average admittances $\bar{\beta}_y$ and $\bar{\beta}_z$ may be obtained by integrating equations (12) over the appropriate intervals. The result for the x - y walls is

$$\bar{\beta}_y = \frac{i\omega\rho_i c_i}{bP_0} \left[\frac{A_1}{\alpha_1} \sin(\alpha_1 a) - \frac{A_2}{\alpha_1} \cos(\alpha_1 a) + \frac{A_3}{\alpha_2} \sinh(\alpha_2 a) + \frac{A_4}{\alpha_2} \cosh(\alpha_2 a) + \frac{A_2}{\alpha_1} - \frac{A_4}{\alpha_2} \right] + \frac{i\omega\rho_i c_i K}{k_x^4 - \gamma^4}, \tag{19}$$

and the expression for the x - z walls is identical if the A 's are replaced by the B 's, and a by b .

3. COMPUTATION OF RESULTS

Some comments should be made concerning the computational methods used to obtain the numerical results derived from the theory. An obvious procedure would be initially to put k_x equal to k_p , solve equations (13) for the A 's and B 's, calculate $\bar{\beta}$ from equation (19) and its x - z counterpart, obtain a new value of k_x from equation (6) and repeat the procedure with this new value, performing as many iterations as necessary to obtain convergence of the solution for k_x . This procedure cannot be guaranteed always to be successful and so an alternative would be to insert the expression for $\bar{\beta}$ in terms of k_x into equation (6), and obtain an equation of the form $f(k_x) = 0$; the Newton-Raphson iterative method could then be used to obtain a solution for k_x . Neither of these procedures proved to be either practicable or necessary, however, for the following reasons.

Equations (13), as they stand, lead to a set of eight *ill-conditioned* equations in the unknowns A_1 to A_4 and B_1 to B_4 . Attempts were made to solve these by using the Gauss elimination method (including the use of error equations) and by the Gauss-Jordan method. The results were very unsatisfactory, and considerable scatter was encountered. Next, the slope of the duct walls at the corners was inserted as an unknown in equations (13), and a set of nine equations was obtained; this time, only one of equations (13g) and (13h) was required. The resultant set of equations proved to be much more amenable to solution, although a small amount of scatter still occurred, mainly at low frequencies. The accuracy of solution was not such as to enable either of the iterative procedures described above to be used successfully.

If one examines the values of γ and k_i for typical air conditioning ductwork, it transpires that γ is about an order of magnitude higher than k_p , so provided k_x is not too much *greater* than k_p , then values of α_1 , α_2 and $(k_x^4 - \gamma^4)$ would contain extremely small errors if k_i were used to obtain values for $\bar{\beta}$, and also of course, $\bar{\beta}$ would be quite accurate. The condition of k_x being too much greater than γ would only occur when the duct walls were too transparent to sound for the theory to be applicable in any case, and so no real problem ensues from the above approximation. Once $\bar{\beta}$ has been calculated, more accurate values of k_x may of course be obtained from equation (6); these are necessary in order to calculate C_r and the TL .

The TL (and other quantities such as wall mode shapes and c_w) were calculated as outlined above, and reasonably satisfactory results were obtained. No doubt further work on re-arrangement of the equations and other means of solution would yield better results, but this was not felt to be merited in the present investigation. Incidentally, for square ducts, the problems over accuracy of solution did not arise, but this is almost irrelevant in the general context of rectangular duct shapes.

The effects of internal damping were investigated initially for a square duct, but proved to be negligible even for relatively large values of η . Subsequently the computer program used was re-written, incorporating only real (as opposed to complex) variables, with an attendant improvement in accuracy.

4. MEASUREMENTS

In order to test the theory, two experimental rigs were constructed. These are shown in Figure 4. The first, in Figure 4(a), consisted of a square duct with a loudspeaker (as an acoustic source) at one end, and was anechoically terminated by a wedge of Rockwool, which not only acted as an effective acoustic absorber but also damped the wall vibrations progressively. This arrangement was designed to approximate to the idealized situation where waves travel, in one direction only, along a duct of finite length. In order to ameliorate

the effects of structural discontinuities, all seams in the duct wall were butt-welded and beaten flat. Near field effects close to the loudspeaker, and phenomena caused by the non-ideality of the termination would, it was hoped, be negligible. Provision was made to carry out axial traverses of the sound field with a probe microphone.

The second duct, shown in Figure 4(b), was rectangular (not square) in section, again having the loudspeaker as a source, but with a termination consisting of a metal flange bearing a rigid plate (of aluminium, heavily weighted and damped with putty). This was

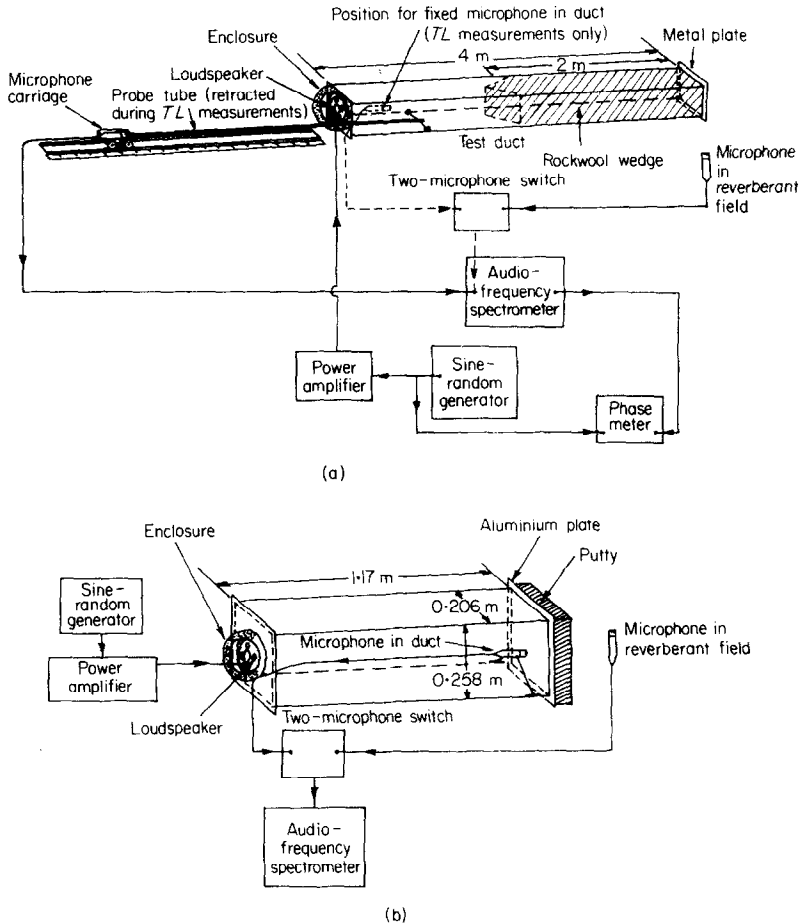


Figure 4. Experimental arrangements. (a) Square duct with anechoic termination; (b) rectangular duct with reflecting termination.

intended to act as an extreme test of the theory, because of the presence of reflected structural and acoustic waves, and also because the ratio between the length of the duct and its greater transverse dimension was relatively small compared to most practical ducts (so "end effects" would perhaps be more noticeable). Additionally, the duct had a lapped, riveted seam on one side along the whole of its length.

Extraneous transmission of sound from the back of the loudspeaker was reduced to negligible proportions by means of a massive double-walled enclosure with sand in the cavity; acoustic resonances between this and the speaker were damped by using acoustic absorbent. This arrangement proved to be quite satisfactory. The anechoic termination in

the square duct was also effective; Figure 5 shows some typical axial sound pressure patterns measured inside the duct. Even at 124 Hz, the standing-wave ratio is only 7 dB (representing an energy reflection coefficient of approximately 0.15), and this falls to 1 dB or less at higher frequencies. As far as the effectiveness of the anechoic termination in terms of structural waves is concerned, the situation appears complicated. Axial, structural, "standing-wave" patterns were detected, but interpretation proved difficult. The separation of the displacement nodes was generally considerably smaller than that in the coupled wave system, and

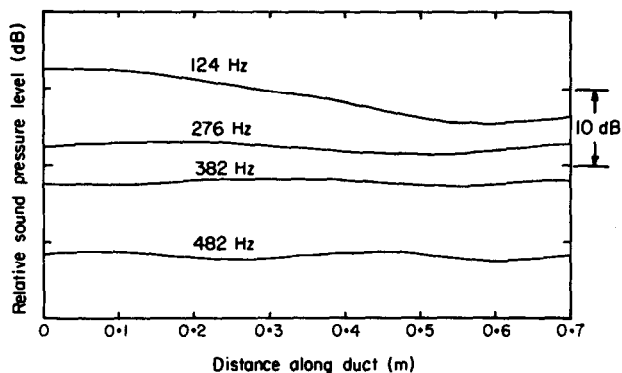


Figure 5. Axial sound pressure patterns in the square duct.

was not very regular. Whether these displacement patterns can be attributed to structural reflection from the anechoic termination or to effects caused by reflections at the welded joints in the duct is a moot point, but at all events, the reflections were of small magnitude. At 245 Hz, for example, the standing wave ratio was about 5 dB, and the separation of displacement minima was of the order of 0.2 m.

Measurements of the wall TL were made on these ducts in $\frac{1}{3}$ octave frequency bands: wide band noise was fed to the loudspeaker, and passed from the detecting microphones to a $\frac{1}{3}$ octave band audio-frequency spectrometer. The sound pressure level (L_p) inside the duct was measured with a fixed microphone; with the duct in Figure 4(b), this was placed close to the end-plate so as to measure the maximum axial sound pressure level at all frequencies. This would give a measurement about 3 dB higher than the L_p based upon the sum of the incident and reflected mean square acoustic pressures (this quantity was taken to be the appropriate L_p to be used in TL calculations, since it is related to the sum of the absolute values of incident and reflected sound power), and accordingly 3 dB was subtracted from the internal L_p in this case. The internal sound power was determined by adding $10 \log(abc/c_x)$ to the internal L_p (calculated values of c_x were used). The radiated sound power level was measured by the source substitution method, with a standard source of known sound power output, and by utilizing the laboratory as a "reverberant room".

Acoustic phase velocity (equal to radian frequency divided by phase change per unit distance) and axial sound pressure level distribution measurements were made in the square duct with the probe microphone. Wall vibration amplitude measurements, which yielded transverse displacement patterns, were made on both the square and rectangular ducts, by using an extremely small Endevco accelerometer (model no. 22) in conjunction with an Endevco charge amplifier (type 2730), whose output was fed to the audio-frequency spectrometer. The accelerometer was so light that it did not cause significant "mass-loading" of the vibrating duct wall.

The results of the various measurements are described in the next section.

5. COMPARISON BETWEEN EXPERIMENT AND THEORY

It is convenient to subdivide this discussion into two parts, the first appertaining to the square duct and the second to the rectangular duct.

5.1. SQUARE DUCT

The square duct was constructed of mild steel with $h = 1.219$ mm, $E = 2.119 \times 10^{11}$ Pa, $m = 9.63$ kg/m², $\sigma = 0.291$, $a = 0.203$ m and $b = 0.203$ m, and had an effective radiating length of 2.1 m.

Figure 6 shows typical calculated and measured displacement profiles on one of the walls,

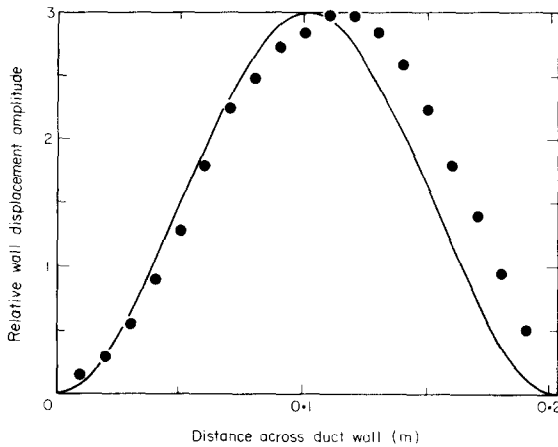


Figure 6. Displacement profile on a wall of the square duct. ●, Measurements; —, theory; $f = 277.3$ Hz.

at 277.3 Hz; only relative, not absolute values were compared. The general shapes of the curves are similar, although the peak in the measured values is displaced from the centre, presumably because of slight (inevitable) asymmetry in the duct's construction. The calculated curve shows zero slope at the duct's corners. This is because the duct's walls are all of equal width, vibrate similarly, and thus the boundary conditions at the edges of each wall are effectively 'built-in', since the corners are assumed to remain right-angled; this argument obviously applies only to square section ducts.

The calculated and measured axial phase speed, c_x , of the wave is shown as a function of frequency in Figure 7 (the calculated values were obtained by using equation (19)). One sees that the phase speed is subsonic below about 170 Hz and supersonic between that frequency and 850 Hz (the upper limit of the calculated curve); at frequencies near to, but less than 170 Hz, c_x drops sharply as the frequency rises, while just above 170 Hz, c_x rises rapidly as the frequency falls. This behaviour indicates that a wall resonance is occurring at around 170 Hz. At frequencies above about 300 Hz, c_x approaches c_e ($=c_p$, since the duct contained air). There is good agreement between predictions and measurements of c_x , even close to the resonance, where the theory might have been expected to give poor results because of neglect of the external radiation load on the duct walls.

The calculated average wall admittance, β , is shown in Figure 8. A loss factor of 0.002 was taken for the duct wall material, resulting in a (small) real, as well as an imaginary,

part to the admittance. (In reality though, radiation losses would probably swamp the conductance caused by internal damping, but these losses, of course, were not taken into account.) One sees evidence again, of a resonance at around 170 Hz.

It is also of interest to note how the radiation efficiency, C_r , varies with frequency. Figure 9 shows theoretical results based on the calculated phase speed and Brown and Rennison's line source model. One sees that in regions where $c_x \approx c_e$, the radiation efficiency is, as expected, 3 dB less than that for an infinite line source with supersonic phase speed, but that for large values of c_x (at frequencies just above resonance), this difference tends to zero.

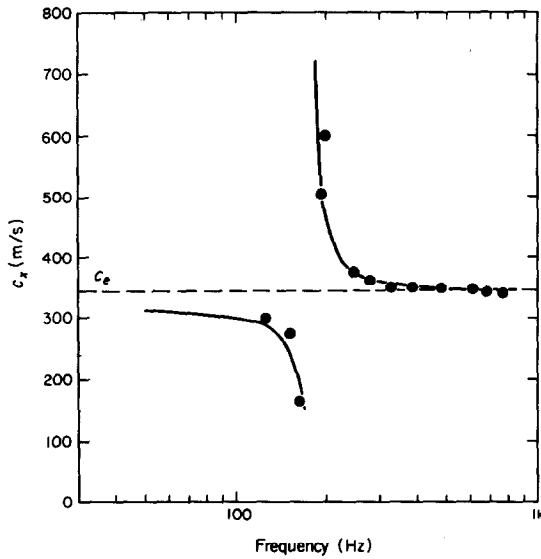


Figure 7. Axial phase speed in the square duct. ●, Measurements; —, theory.

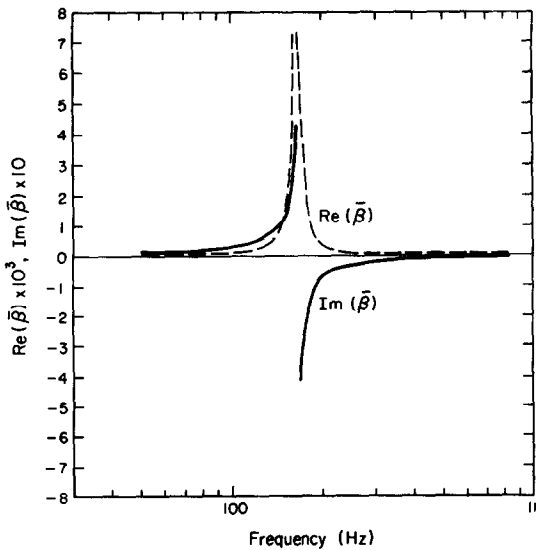


Figure 8. Calculated average wall admittance in the square duct.

On the other hand, for small values of c_x , the radiation efficiency can fall significantly, and this occurs at frequencies just below resonance.

The most important comparison between prediction and measurement is, of course, in the transmission loss, and Figure 10 shows the third-octave measurements of TL , compared to a theoretical curve from equation (18). The “cut-on” frequency for the (0, 1) and (1, 0) modes is also indicated.

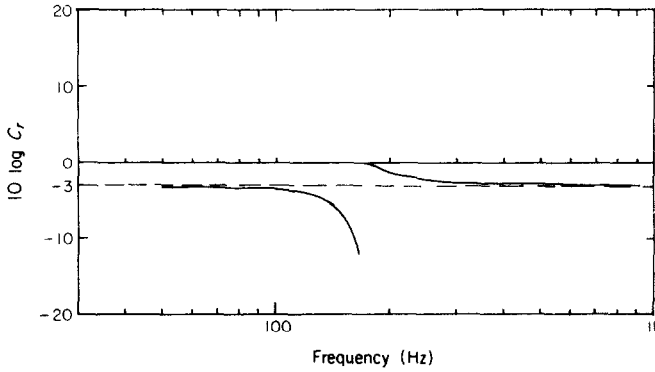


Figure 9. Radiation efficiency of the square duct.

acoustic modes in the equivalent rigid-walled duct is also indicated. Agreement between the measurements and theory is very good up to a frequency of about two-thirds the cut-on frequency for the lowest order cross-modes. The most obvious feature of the TL curve is that it falls to a sharp minimum at about 170–180 Hz. This corresponds to the duct wall resonance mentioned previously. Because of the fact that, in the special case of a square duct, the corners are effectively built-in, a comparison may be made with the equivalent “transverse beam” duct wall resonances. That is, one may imagine a transverse strip of the duct wall acting as a beam with built-in ends, and consider its natural frequencies of vibration. The fundamental frequency of such a beam is shown in Figure 10, and this was calculated by using results of Warburton [8]. The frequency is quite close to the measured and predicted duct wall resonant frequency, and this seems to show that the resonance is essentially of a transverse type. That the axial wavenumber is non-zero does, of course, make this view

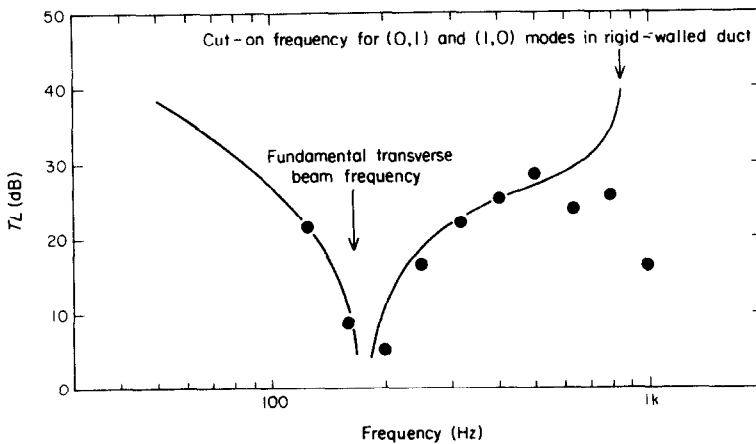


Figure 10. Wall transmission loss of the square duct. ●, Measurements; —, theory.

simplistic to an extent, although only inasmuch as the "twisting" motion imposed upon the (imaginary) beam by the longitudinal wave motion in the duct is neglected.

The deterioration in agreement between theory and measurements at higher frequencies is almost certainly caused by two factors: first, the increasing non-uniformity (with rising frequency) of transverse acoustic pressure in the duct, and secondly the breakdown of the simple line source model when a transverse duct dimension approaches an acoustic wavelength. On the basis of these ideas, one may state, tentatively, that the present model would normally be satisfactory up to about two-thirds of the cut-on frequency of the lowest higher-order mode in the equivalent rigid-walled duct; the upper frequency limit for validity of the theory should therefore "scale" with the duct cross-section. It is clear too, though, that the effects of non-uniformities in transverse pressure distribution caused by wall resonances, if superimposed upon impending higher-order mode transmission phenomena, could cause a lowering of this upper frequency limit.

5.2. RECTANGULAR DUCT

The rectangular duct was constructed of "18 gauge" galvanized steel, typical of that used in air conditioning ductwork. Its transverse dimensions were $a = 0.206$ m and $b = 0.258$ m. Because of the zinc coating on either side of the inner mild steel sheet, an effective value of E had to be calculated as $E_{\text{eff}} = [E_1 h_1^3 + 6E_2(h_1 + h_2)^2 h_2]/(h_1 + 2h_2)^3$, where h_1 is the thickness of the steel sheet (1.219 mm), h_2 is the thickness of galvanizing on either side (0.076 mm), E_1 is the Young's modulus of mild steel (2.119×10^{11} Pa) and E_2 is the Young's modulus of zinc (1.084×10^{11} Pa). The value of E_{eff} in this case was 1.816×10^{11} Pa. The mass per unit area was calculated by adding the mass per unit area of the steel sheet to those of the zinc coatings and was equal to 10.72 kg/m².

Figure 11 shows calculated and measured displacement amplitude patterns, and also the

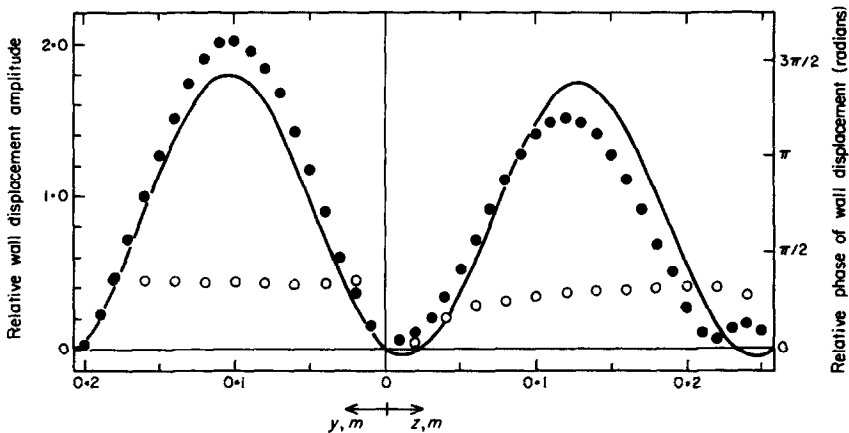


Figure 11. Wall displacement and phase profiles on the rectangular duct. ●, Measurements of displacement; ○, measurements of phase; —, theoretical displacement profile; $f = 246$ Hz.

measured phase, on two of the duct's walls at 246 Hz. Again, no attempt is made to predict absolute values of displacement, although in both the measurements and the theoretical curve the correct relative displacement amplitude is maintained between the two duct walls. One sees that the agreement between experiment and theory is fair, especially in view of the non-ideality of the duct engendered by the seam along one of its walls. The small regions

(appearing in the theoretical curve) along the edges of the x - z walls, with opposite phase to the x - y wall vibrations, are not evident in the amplitude measurements, although the measured phase does show a tendency to change near to the corners. An additional reason for discrepancies between prediction and measurement may be that the ducts on which the experiments were carried out did not, by virtue of their means of construction, have sharply right-angled corners, but had slightly rounded ones, whereas it was assumed in the theory that the corners were sharp.

To illustrate more clearly the effects of rotation of the corners on the displacement pattern of the duct walls, a theoretical curve is included here for a frequency where the rotation is quite pronounced, and this is shown in Figure 12; the frequency is 560 Hz. The corners may

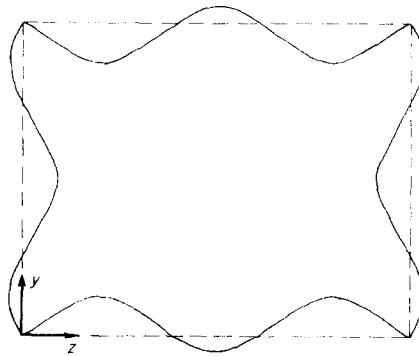


Figure 12. Calculated wall displacement profile on the rectangular duct. $f = 560$ Hz.

be seen to remain right-angled and the displacement pattern is symmetrical, as stated in section 2.5. Although some volume velocity “cancellation” on each wall occurs, this is only partial, and the net volume velocity is actually in the same direction (that is, inward or outward) on all walls.

As with the square duct, the feature of most interest with the rectangular configuration is the transmission loss, and Figure 13 compares theoretical and measured values. Once again, these agree quite well up to about $\frac{2}{3}$ of the cut-on frequency for the $(0, 1)$ mode, although at the lowest frequency of measurement—125 Hz—some discrepancy is evident. It seems likely that here, where the wavelength of the structural/acoustic wave is somewhat greater than the length of the duct, “end effects” at the (reflecting) duct termination would prevent the predicted wall resonances, characteristic of an infinite duct, from realising their full effect in lowering the wall TL .

This good agreement between prediction and measurement is rather surprising in view of the wide discrepancies between theoretical assumptions and experimental conditions, but it is consistent with the findings of Brown and Rennison for circular ducts, in that a theory which accounts for only a *single* travelling wave also gives good predictions for a system where strong reflected waves are present. A thorough explanation of this could, one supposes, only be made on the basis of a more complete theory than that given here, but it may be speculated that the radiated sound power may be computed as the sum of the powers from incident and reflected waves, as is the case with an infinite duct along which waves travel faster than the external adiabatic speed of sound.

Although the theoretical curve in Figure 13 shows evidence of wall resonances, it would be meaningless, in general, to try to explain these in terms of “classical” transverse beam resonances, since the boundary conditions are not built-in, simply supported, or free:

accordingly, no such attempt will be made, and it is sufficient to say that these resonances are, again, presumably transverse in nature, although less easily explicable than those in the square duct.

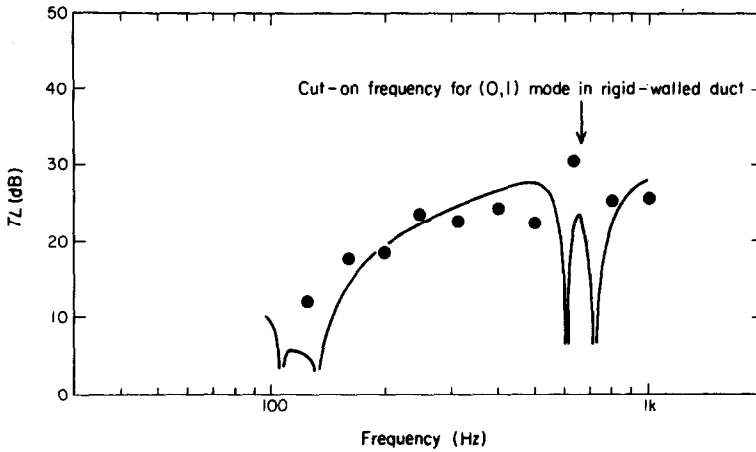


Figure 13. Wall transmission loss of the rectangular duct. ●, Measurements; —, theory.

6. DISCUSSION AND CONCLUSIONS

One of the problems associated with noise radiation from rectangular ducts—particularly those in air-moving systems—has been isolated, namely that of low frequency acoustic “breakout”. A simple theory for predicting the sound transmission loss of duct walls at low frequencies has been described, and shown to give good agreement with measurements on two different duct systems, one of which was deliberately designed as an extreme test of the theory.

It seems reasonable to conclude, in view of the preceding arguments, that the theory described here should generally give reliable predictions of duct wall transmission loss up to about $\frac{2}{3}$ of the cut-on frequency for the lowest cross-mode in the equivalent rigid-walled duct.

At present, there would seem to be some difficulty associated with producing design charts for duct wall sound transmission loss. The vibrational interaction between a duct’s walls governs the shape of the transmission loss curve and cannot be predicted, it appears, by any procedure easier than that of actually solving the equations of motion for the walls; it also depends upon the aspect ratio of the duct’s cross-section, and would vary in what is probably not a very simple manner between individual cases. Additionally, the transmission loss has what are apparently rather complicated “scaling laws” between its various controlling factors such as duct wall thickness and dimensions. So it does not look as if one would easily be able to produce the equivalent of the existing charts, for calculating the *TL* of a flat single panel, which are based upon infinite panel theory. It may well be, however, that this problem would merit further pursuit, although it is not the purpose of the present investigation to do this.

Further work would also be useful on means of improving wall transmission loss, such as wall stiffening, the addition of damping material, and the application of external lagging. The present results should assist in creating a basis for such investigations, and it is intended that these will be carried out. Additionally, a knowledge of the effects of bends on duct wall

transmission loss, and also of the relative importance of turbulent, as opposed to acoustic excitation mechanisms, would be enlightening, although the associated theoretical analyses and indeed, experimental measurement procedures, would probably be considerably more complicated than those described in this article.

ACKNOWLEDGMENTS

The author is indebted to Dr C. L. Morfey, of the Institute of Sound and Vibration Research at the University of Southampton, for helpful comments, and gratefully acknowledges the loan of vibration measuring equipment from the Scientific Services Department of the Central Electricity Generating Board at Gravesend.

REFERENCES

1. J. D. WEBB 1972 *Noise Control in Mechanical Services*. Colchester: Sound Attenuators Ltd., Sound Research Laboratories Ltd. See chapter 9.
2. L. CREMER 1955 *Acustica* **5**, 245–256. Theory of sound transmission through cylindrical shells. (In German.)
3. M. HECKL 1958 *Acustica* **8**, 259–265. Experimental investigation of sound transmission through cylinders. (In German.)
4. C. L. MORFEY 1971 *Proceedings of the Seventh International Congress on Acoustics, Budapest, Paper 24 A9*. Transmission through duct walls of internally-propagated sound.
5. G. L. BROWN and D. C. RENNISON 1974 *Proceedings of the Noise, Shock and Vibration Conference, Monash University, Melbourne*, 416–425. Sound radiation from pipes excited by plane acoustic waves.
6. G. F. KUHN and C. L. MORFEY 1976 *Journal of Sound and Vibration* **47**, 147–161. Transmission of low-frequency internal sound through pipe walls.
7. C. H. ALLEN 1960 *Noise Reduction* (Editor L. L. Beranek). New York: McGraw-Hill. See chapter 21.
8. G. B. WARBURTON 1954 *Proceedings of the Institution of Mechanical Engineers* **168**, 371–384. The vibration of rectangular plates.

APPENDIX: LIST OF SYMBOLS

A_1 to A_4 ,	coefficients in expressions for duct wall displacement	h_1, h_2	thicknesses of central and outer layers (respectively) of a galvanized metal sheet
B_1 to B_4	transverse dimensions of duct wall in y and z directions respectively	i	$\sqrt{-1}$
a, b	radiation efficiency of a line source or duct	K	a constant, dependent upon the duct wall material
C_r	adiabatic speed of sound	k	a wavenumber
c	displacement amplitude	L	perimeter of duct cross-section
D	Young's modulus	l	radiating length of duct
E	Young's moduli of central and outer layers (respectively) of a galvanized metal sheet	L_p	sound pressure level
E_1, E_2	effective Young's modulus of a galvanized metal sheet	m	mass per unit area of duct wall
E_{eff}	base of the natural logarithm	P_0	acoustic pressure amplitude
e	frequency	p	acoustic pressure
f	denotes a function of a single variable w	Q	a pressure amplitude
$f(w)$	thickness of duct wall	q	a pressure
h		S	cross-sectional area of duct
		s	circumferential co-ordinate on duct wall
		t	time

u	acoustic particle velocity	λ	propagation coefficient
W_{int}	sound power transmitted inside duct	ξ	transverse displacement of duct wall
W_{ext}	radiated sound power per unit length of duct	ρ	time-averaged density of a fluid, or else acoustic density fluctuation
x	axial spatial co-ordinate in duct	σ	Poisson's ratio
y	transverse spatial co-ordinate in duct	ω	radian frequency
$Y(y)$	y -dependent factor in an expression for duct wall displacement	∇^2	two-dimensional Laplacian operator, either $\partial^2/\partial x^2 + \partial^2/\partial y^2$ or $\partial^2/\partial x^2 + \partial^2/\partial z^2$
z	transverse spatial co-ordinate in duct	∇^4	operator, $\equiv (\nabla^2)^2$
$Z(z)$	z -dependent factor in an expression for duct wall displacement	$ w $	denotes the modulus of a complex quantity w
α_1, α_2	structural wavenumbers	<i>Subscripts</i>	
β	duct wall admittance	e	denotes a quantity outside the duct
$\bar{\beta}, \bar{\beta}_y, \bar{\beta}_z$	duct wall admittance averaged over the whole duct perimeter, in the y direction, in the z direction, respectively	i	denotes a quantity inside the duct
γ	a quantity with the dimensions of, and resembling, a wavenumber	0	denotes the amplitude of a time-varying quantity
Δx	axial thickness of a fluid element in a duct	x	denotes the component of a vector in the x direction
η	internal damping factor, or "loss factor" of wall material	<i>Superscripts</i>	
			denotes differentiation of a function with respect to its argument